Chemistry & Biology, Vol. 9, 1237–1245, November, 2002, ©2002 Elsevier Science Ltd. All rights reserved. PII S1074-5521(02)00268-5

# Characterization of a Specificity Factor for an AAA+ ATPase: Assembly of SspB Dimers with ssrA-Tagged Proteins and the ClpX Hexamer

**David A. Wah,[1] Igor Levchenko,[1,2] Tania A. Baker,[1,2] and Robert T. Sauer[1,3]**
[1]Department of Biology
[2]Howard Hughes Medical Institute
Massachusetts Institute of Technology
Cambridge, Massachusetts 02139

## Summary

**SspB, a specificity factor for the ATP-dependent ClpXP protease, stimulates proteolysis of protein substrates bearing the ssrA degradation tag. The SspB protein is shown here to form a stable homodimer with two independent binding sites for ssrA-tagged proteins or peptides. SspB by itself binds to ClpX and stimulates the ATPase activity of this enzyme. In the presence of ATPγS, a ternary complex of SspB, GFP-ssrA, and the ClpX ATPase was sufficiently stable to isolate by gel-filtration or ion-exchange chromatography. This complex consists of one SspB dimer, two molecules of GFP-ssrA, and one ClpX hexamer. SspB dimers do not commit bound substrates to ClpXP degradation but increase the affinity and cooperativity of binding of ssrA-tagged substrates to ClpX, facilitating enhanced degradation at low substrate concentrations.**

## Introduction

Many intracellular proteases consist of a multisubunit peptidase with active sites sequestered in an internal chamber and an associated AAA+ ATPase that binds, unfolds, and translocates specific protein substrates into the proteolytic chamber [1, 2]. The eukaryotic and archaebacterial 26S proteasomes and the eubacterial ClpXP, ClpAP, and HslUV proteases are ATP-dependent intracellular enzymes that share this basic structural organization and mechanism [3–10]. Interactions mediated by the AAA+ ATPase determine the degradation specificity of these energy-dependent proteases for some substrates. For example, the ClpX ATPase of the *Escherichia coli* ClpXP protease binds distinct peptide sequences displayed on otherwise native proteins [11–15]. One such ClpX-targeting sequence is the ssrA tag (AANDENYALAA), which is cotranslationally added to nascent polypeptides when ribosomes stall [16, 17]. Proteins bearing the ssrA tag at their C termini are bound by ClpX hexamers, denatured, and translocated into ClpP for degradation [13, 18–20].

Additional factors also play important roles in regulating proteolytic specificity and flux. For example, the SspB protein stimulates degradation of ssrA-tagged substrates by ClpXP but inhibits degradation of these same substrates by the related ClpAP protease [21, 22]. ClpS acts as a substrate modulator for ClpAP by directing degradation toward protein aggregates and inhibiting degradation of ssrA-tagged substrates [23]. RssB is required for ClpXP-mediated degradation of the $\sigma^S$ transcription factor [24, 25]. The *Bacillus subtilis* protease ClpCP requires the specificity factor MecA to degrade proteins involved in the regulation of the development of competence [26]. In eukaryotes, the p97 ATPase associates with the protein factors p47, Udf1p, and Npl4 to promote different intracellular processes [27–30].

What macromolecular interactions are required for the activity of accessory factors such as SspB, which function to modulate specificity and stimulate degradation? It is known that SspB recognizes residues in the N-terminal portion of the ssrA tag, whereas ClpX recognizes the C-terminal residues of the tag [21, 22]. In principle, SspB might bind ssrA-tagged substrates transiently, modifying them for subsequent interactions with ClpX. Alternatively, macromolecular complexes of SspB, ssrA-tagged substrates, and ClpX might be needed for stimulation of ClpX activity. Here, we show that SspB is a stable homodimer that binds two molecules of a peptide containing the ssrA degradation tag or GFP-ssrA. SspB also associates with ClpX and stimulates its ATP hydrolysis activity in the absence of an ssrA-tagged substrate. A ternary complex consisting of one SspB dimer, two molecules of GFP-ssrA, and one ClpX hexamer assembles stably in the presence of the ATPγS. SspB does not commit bound substrates to ClpXP degradation, but acts largely to stabilize the equilibrium binding of ssrA-tagged substrates to the protease and increase the cooperativity of binding. These results help clarify how specificity factors and modulators act selectively in directing substrates to the AAA+ ATPases.

## Results

### Native SspB Is a Stable Dimer

As determined by MALDI-TOF mass spectroscopy, purified *E. coli* SspB protein had a monomer molecular weight (18.3 kDa) within error of the value calculated from its amino acid sequence. In equilibrium analytical ultracentrifugation experiments performed at an initial subunit concentration of 66 μM, SspB sedimented with a mean molecular weight of 35.0 kDa (Figure 1A), a value close to that expected for a dimer. Similar results were obtained in sedimentation experiments performed at protein concentrations of 2.5, 10, 25, and 41 μM. SspB also behaved as a stable dimer in dynamic light-scattering experiments (D = 4.6 F; apparent $M_R$ = 40.6 kDa).

The fluorescence spectrum of native SspB was blue-shifted compared to the spectrum under denaturing conditions, suggesting hydrophobic burial of $Trp^{17}$, the only tryptophan residue in SspB (Figure 1B, inset). Denaturant-induced unfolding of SspB occurred in a cooperative and reversible fashion with a half-maximal $C_m$ value between 3 and 4 M GuHCl as monitored by fluorescence (Figure 1B) or circular dichroism (data not shown). The denaturation $C_m$ increased with SspB concentration

[3]Correspondence: bobsauer@mit.edu

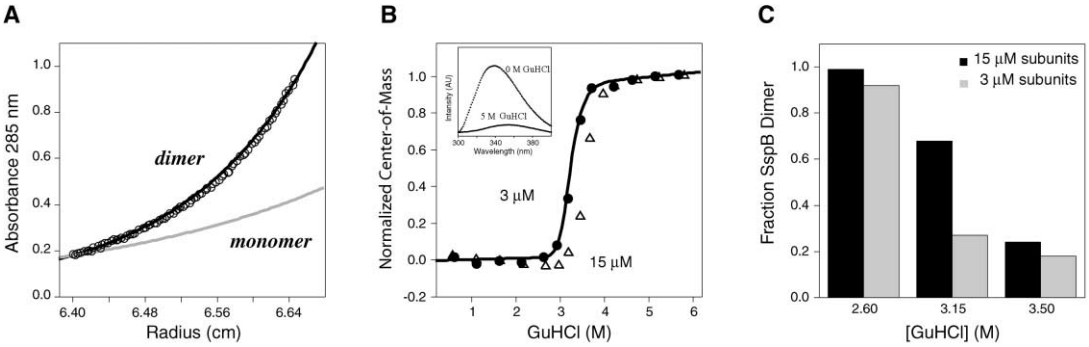


Figure 1. Biophysical Properties of SspB

(A) Equilibrium analytical centrifugation of 41 μM SspB (16,000 rpm, 20°C). The fitted line corresponds to a molecular weight of 35.1 kDa (36.5 kDa expected for SspB dimer). The gray line corresponds to the expected distribution for an SspB monomer (18.3 kDa).

(B) GuHCl stability (25°C) of SspB at concentrations of 3 μM (closed circles) and 15 μM (open triangles) assayed by fluorescence. The solid line is a fit of the 3 μM data, assuming an equilibrium between unfolded monomers and folded dimers ($\Delta G = 27.0$ kcal/mol; $m = 6.0$ kcal/mol•M). The inset shows the fluorescence spectra of 15 μM SspB with or without 5 M GuHCl. The buffer for both experiments was 25 mM Tris-HCl (pH 7.6), 200 mM KCl, and 5% glycerol.

(C) SspB monomer and dimer populations were calculated from analytical ultracentrifugation runs of SspB at concentrations of 3 μM and 15 μM in the buffer described in (B) above plus 2.60, 3.15, or 3.50 M GuHCl. A two-species fit using the molecular weights of SspB monomers and dimers was used to calculate dimer and monomer populations.

(Figure 1B). This result and equilibrium sedimentation experiments (Figure 1C) show that native SspB dimers persist into the denaturation-transition zone. Hence, native SspB dimers are quite stable to both dissociation and denaturation.

### SspB Binding to ClpX and to ssrA-Tagged Peptides and Proteins

Using a coupled assay, we measured steady-state ATP hydrolysis by ClpX in the presence of increasing amounts of SspB. As shown in Figure 2A, SspB stimulated the ATPase activity of ClpX by roughly 2-fold, with half-maximal stimulation occurring at an SspB concentration of ~1 μM at 30°C. Purified SspB had no ATPase activity (data not shown). Hence, SspB and ClpX can interact in the absence of ssrA-tagged peptides or proteins. Moreover, this interaction alters the enzymatic properties of ClpX.

Previous studies have shown that SspB binding to ssrA-tagged proteins can be eliminated by tag mutations and have established that the ssrA tag is both necessary and sufficient for binding [21, 22]. A synthetic peptide (NKKGRHGAANDENYALAA) with seven N-terminal residues chosen to improve peptide solubility and 11 C-terminal residues corresponding to the ssrA tag was synthesized and binding was monitored by isothermal titration calorimetry (ITC). Experiments at 20°C with SspB as the injectant (Figure 2B; Table 1) or the peptide as the injectant (data not shown) were consistent with independent and identical binding of two ssrA peptides to the SspB dimer with a microscopic $K_D$ of 300 ± 20 nM for each binding site.

Data from ITC experiments using SspB and GFP-ssrA showed independent binding of two molecules of GFP-ssrA to the SspB dimer with a $K_D$ of 16 ± 4 nM (Table 1). Hence, SspB binding to GFP-ssrA was approximately 20-fold tighter than binding to the ssrA-peptide. The thermodynamic parameters for these binding interactions are listed in Table 1. A mixture of SspB (6 μM in subunit equivalents) and GFP-ssrA (6 μM in monomer equivalents) was subjected to equilibrium analytical ultracentrifugation (Figure 2C). These data suggested that more than 90% of the molecules had an average molecular weight of 93.2 kDa (the value expected for an $S_2G_2$ complex). Complexes of SspB and GFP-ssrA also migrated near the position expected for an $S_2G_2$ tetramer in gel-filtration experiments (see below).

To establish a more convenient solution binding assay, we labeled the ssrA peptide with a fluorescent BODIPY dye and monitored binding of the modified peptide to SspB by fluorescence anisotropy. The data from experiments at 20°C gave a $K_D$ of 400 ± 50 nM (data not shown). Unmodified peptide competed efficiently for binding ($K_I = 440$ nM), showing that the BODIPY dye is not a significant participant in the binding reaction and validating the use of this assay to monitor SspB-peptide interactions. As discussed below, ClpX also bound to the BODIPY-labeled ssrA peptide ($K_D = 1.2 \pm 0.2$ μM; 20°C), demonstrating as expected that the ssrA tag provides a binding site for ClpX.

### ClpX, SspB, and GFP-ssrA Form a Stable Ternary Complex

The GFP fluorophore absorbs at 500 nm, providing a convenient assay of its elution position during gel-filtration chromatography. As shown in Figure 3A, GFP-ssrA by itself or in $S_2G_2$ complexes eluted from a Superdex 200 column at distinct positions expected for the relative sizes of these species. Chromatography of a mixture of GFP-ssrA, SspB, ClpX, and ATPγS revealed a larger ternary complex (Figure 3A). Chromatography of ternary complexes purified by gel filtration on a reverse-phase C4 HPLC column confirmed the presence of GFP-ssrA, SspB, and ClpX (data not shown). Stable formation of

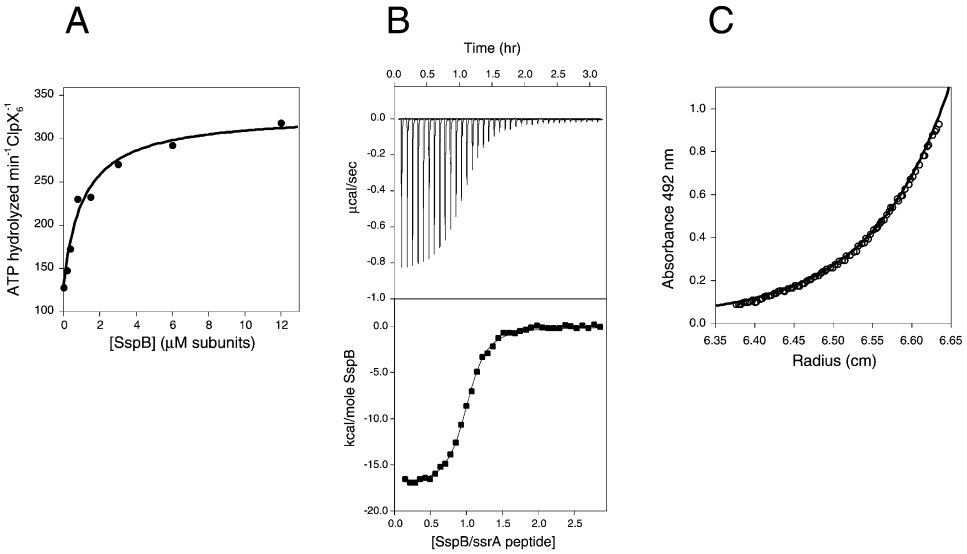


Figure 2. SspB Binding to ClpX and to ssrA-Tagged Peptides and Proteins

(A) SspB stimulation of ClpX-catalyzed ATP hydrolysis (30°C). The fit is a bimolecular binding isotherm with half-maximal stimulation at an SspB concentration of 1.1 ± 0.3 μM (subunit equivalents).

(B) SspB binding to the NKKGRHGAANDENYALAA ssrA peptide assayed by isothermal titration calorimetry (25°C). The top panel shows raw data in power versus time. The lower panel shows integrated areas normalized to the molar quantity of SspB injected at each step. The best-fit curve using a single-site model gave a ΔH of −16.9 kcal/mol, a $K_D$ of 0.30 μM, and a binding stoichiometry of 1.02 ssrA peptides to 1.0 SspB subunit (Table 1).

(C) Equilibrium analytical ultracentrifugation (12,000 rpm, 4°C) of a mixture of SspB (6 μM subunit equivalents) and GFP-ssrA (6 μM) monitored by GFP-ssrA absorbance at 492 nm. The fitted line corresponds to a two-species fit in which 90% of the GFP-ssrA is present as a 93.2 kDa complex (expected for $SspB_2$•GFP-$ssrA_2$), and 10% is present as free GFP-ssrA (27.8 kDa).

the ternary complex required ATPγS. In the absence of SspB, almost no GFP-ssrA chromatographed at a position expected for a complex with ClpX even when ATPγS was present (Figure 3A). Hence, formation of a stable interaction between ClpX and GFP-ssrA is dependent on the presence of SspB.

Several experiments were performed to determine the subunit composition of the ternary complex. First, increasing quantities of the ClpX hexamer were added to a mixture of 3 μM SspB dimer and 6 μM GFP-ssrA monomer, and ternary complex formation was assayed by gel filtration in the presence of ATPγS (Figure 3B). As the $ClpX_6$ concentration was increased, there was a roughly linear shift of the GFP-ssrA into the ternary complex until all of the GFP-ssrA eluted in this peak. Analysis of the results of this experiment gave a stoichiometry of 1.7 ± 0.1 GFP-ssrA monomers for each ClpX hexamer in the complex (Figure 3B, inset). In a second experiment, the ternary complex was isolated as a single peak following ion-exchange chromatography on a MonoQ column in the presence of ATPγS (Figure 3C, inset) and peak fractions were subjected to reverse phase chromatography on C4 HPLC column (Figure 3C). Known quantities of GFP-ssrA, SspB, and ClpX were also chromatographed on the C4 column and used to determine the protein concentration of each species in the ternary complex. The stoichiometry determined from this experiment (normalized to an SspB dimer) was 5.5 ClpX subunits, 2.0 SspB subunits, and 2.1 GFP-ssrA subunits. Because ClpX is hexameric [6], the ternary complex appears to contain one ClpX hexamer, one SspB dimer, and two GFP-ssrA monomers.

The molecular weight of the ternary complex was determined directly from hydrodynamic experiments performed using a mixture corresponding to one ClpX hexamer, one SspB dimer, and two GFP-ssrA monomers in the presence of ATPγS. Sedimentation velocity experiments, monitored by GFP-ssrA absorbance at 500 nm, gave an $s_{20,w}$ sedimentation coefficient of 10.8 S when analyzed by the time derivative method [31]. Dynamic light scattering gave a $D_{20,w}$ translation diffusion coefficient of 2.64 F for the complex. The molecular mass calculated from the $s_{20,w}$ and $D_{20,w}$ values was 377 ± 34 kDa (Table 2), within error of the value of 370 kDa

Table 1. Thermodynamics of SspB Interactions with ssrA Peptide and GFP-ssrA at 25°C by Isothermal Titration Calorimetry

| Proteins | $\Delta G^\circ$ (kcal/mole, monomer equivalents) | $\Delta H^\circ$ (kcal/mole, monomer equivalents) | $-T\Delta S^\circ$ (kcal/mole, monomer equivalents) | $K_D$ (nM) | $n$ (monomers) |
|---|---|---|---|---|---|
| SspB•ssrA-peptide | −8.9 | −16.9 | 8.0 | 300 | 1.02 |
| SSpB•GFP-ssrA | −10.6 | −14.1 | 3.5 | 16 | 1.07 |

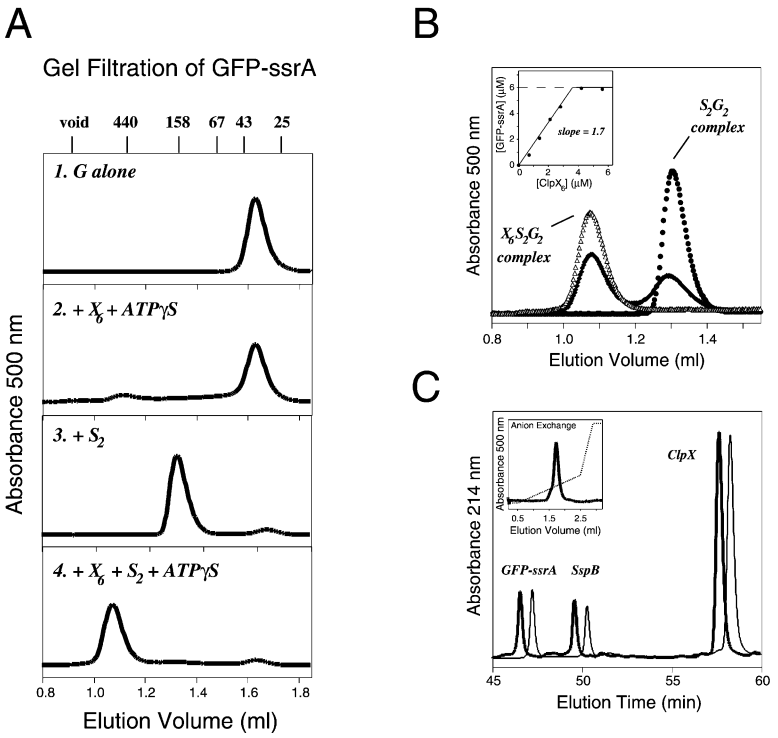


Figure 3. Isolation and Stoichiometry of a Complex of ClpX, SspB, and GFP-ssrA

(A) Superdex-200 gel filtration at 4°C in the presence of 1 mM ATPγS in the elution buffer of (*1*) GFP-ssrA (6 μM), (*2*) GFP-ssrA (6 μM) plus $ClpX_6$ (8 μM), (*3*) GFP-ssrA (6 μM) plus $SspB_2$ (3 μM), and (*4*) GFP-ssrA (6 μM) plus $SspB_2$ (3 μM) plus $ClpX_6$ (8 μM). Note that only the elution position of the GFP-ssrA is detected by absorbance at 500 nm. The positions of molecular weight standards in kDa are marked at the top of the panel.

(B) Gel filtration as shown in (A) for 3 μM $SspB_2$, 6 μM GFP-ssrA plus 5.6 μM $ClpX_6$ (open triangles), 2.8 μM $ClpX_6$ (closed diamonds), or no $ClpX_6$ (closed circles). For these and additional experiments, the inset shows the quantity of GFP-ssrA present in the $X_6S_2G_2$ complex as a function of the quantity of added $ClpX_6$. The slope of the fitted line shows that roughly 1.7 GFP-ssrA molecules are bound to each $ClpX_6$•$SspB_2$ in the ternary complex.

(C) Reverse-phase HPLC separation of proteins in the ternary complex. The black curve shows the peak fractions from anion-exchange purification of the ternary complex (see inset). The gray curve shows chromatography of 0.15 μM $ClpX_6$, 0.33 μM SspB, and 0.34 μM GFP-ssrA for comparison and is offset by 0.5 min for clarity.

calculated for a complex consisting of one ClpX hexamer, one SspB dimer, and two GFP-ssrA monomers. These studies conclusively rule out the possibility that ternary complexes contain more than one ClpX hexamer.

### SspB Enhances ClpX Binding to ssrA-Tagged Peptides

Previous studies have shown that SspB lowers the $K_M$ for GFP-ssrA degradation by ClpXP, suggesting that SspB enhances binding of the ssrA substrate to ClpX [21, 22]. As a test, interaction of the fluorescent BODIPY-labeled ssrA peptide with SspB dimers, ClpX hexamers, or a mixture of SspB dimers and ClpX hexamers was assayed by fluorescence anisotropy. Binding curves at 30°C are shown in Figure 4, left. As expected from their relative molecular weights, the anisotropy at saturating concentrations was higher for the ternary complex than for the ClpX-ssrA peptide complex, which in turn was higher than for the SspB-ssrA peptide complex. Under these conditions, half-maximal peptide binding was observed at a concentration of 2.5 ± 0.6 μM ClpX binding sites (assuming one site per hexamer) or 1.3 ± 0.1 μM SspB binding sites (assuming two sites per dimer). These binding curves showed no cooperativity. In contrast, half-maximal peptide binding was observed at a concentration of 350 ± 40 nM (assuming two sites per $ClpX_6$•$SspB_2$) in the experiment containing both ClpX and SspB, and a Hill constant of 1.8 ± 0.3 was required to fit this binding curve. These results show directly that SspB enhances the binding of the ssrA peptide to ClpX. The positive cooperativity in formation of the ternary complex most likely arises because binary complexes of SspB and the ssrA-tagged peptide are not fully populated at low concentrations but are stabilized by binding ClpX.

As a functional comparison, the rate of ClpXP-mediated degradation of GFP-ssrA at 30°C was assayed with respect to increasing quantities of GFP-ssrA alone or a 1:2 mixture of SspB dimers and GFP-ssrA monomers (Figure 4, right). As expected from previous studies [21, 22], the presence of SspB increased $V_{max}$ and lowered the apparent $K_M$ for degradation of GFP-ssrA. Fitting of the data with SspB, however, required a Hill constant

Table 2. Hydrodynamics of the ClpX-SspB-GFP-ssrA Ternary Complex

| $D_{20,w}$ (Fick) | $s_{20,w}$ (Svedberg) | Calculated Molecular Mass (kDa) | Expected Molecular Mass* (kDa) |
|---|---|---|---|
| 2.64 (2.51–2.82) | 10.7 (10.4–10.9) | 377 (343–404) | 370 |

Diffusion and sedimentation coefficients $D_{20,w}$ and $s_{20,w}$ were determined independently by dynamic light scattering and velocity sedimentation, respectively, and adjusted for conditions of 20°C in water.

*Molecular mass expected for a complex comprising one ClpX hexamer, one SspB dimer, and two GFP-ssrA monomers as calculated from amino acid sequence.

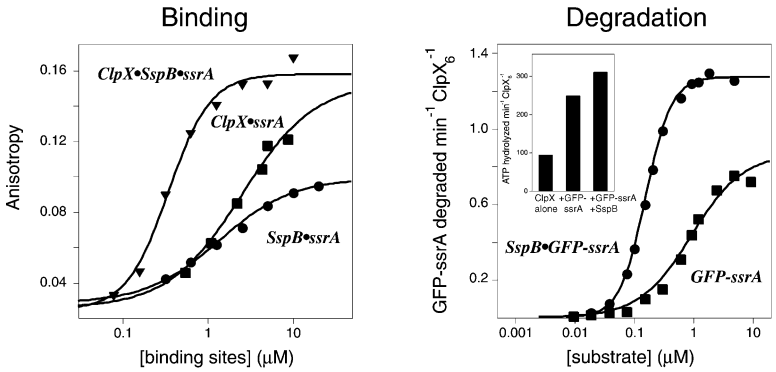


Figure 4. Binding and Degradation of ssrA-Tagged Molecules in the Presence of SspB

Left: binding assayed by fluorescence anisotropy (30°C) of BODIPY-labeled ssrA peptide to SspB, ClpX, or a mixture of SspB and ClpX (1 SspB dimer per ClpX hexamer). The fits of the SspB and ClpX data are to bimolecular reactions. For the mixture of ClpX and SspB, the best fits of the binding data required a Hill constant of 1.8 ± 0.3.

Right: the rate of ClpXP-mediated degradation of GFP-ssrA (30°C) assayed as a function of increasing quantities of GFP-ssrA alone or a mixture of one SspB dimer and two GFP-ssrA monomers. The presence of SspB increased $V_{max}$ and lowered the apparent $K_M$ for degradation of GFP-ssrA. Fitting of the data with SspB required a Hill constant of 1.9 ± 0.1. The inset shows the steady-state ATP hydrolysis rate measured with 0.3 μM $ClpX_6$ alone, in the presence of 10 μM GFP-ssrA, and in the presence of 10 μM subunit equivalents of SspB and GFP-ssrA.

of 1.9 ± 0.1, consistent with the binding data (Figure 4, left) and supportive of the idea that formation of $SspB_2$•GFP-$ssrA_2$ complexes is stabilized by binding to ClpX hexamers.

### SspB Does Not Commit Bound Substrates to Degradation

Because SspB enhances the binding of ssrA-tagged substrates to ClpX, we wondered whether SspB might commit bound ssrA-tagged substrates to enzymatic processing. To test this model, complexes of GFP-ssrA, ClpX, and ClpP were allowed to form in the presence of ATPγS with or without SspB. In one set of reactions, degradation was initiated by adding ATP together with a nonfluorescent competing substrate (Arc-ssrA). In other reactions, the competitor was added before addition of ATP, or no competitor and only ATP was added. In the absence of SspB, GFP-ssrA degradation slowed immediately whether the competitor was added first or added together with ATP (Figure 5, right). Simultaneous addition of ATP and competitor to samples with SspB resulted in an initial rate of GFP-ssrA degradation that was roughly 60% of the rate with no inhibitor, which decayed to the preinhibited rate with a half-life of roughly 60 s (Figure 5, left). Hence, SspB provides some protection against immediate competition by other substrates. Moreover, these results show that some substrates complexed with ClpXP, SspB, and ATPγS can be degraded without having to dissociate and reassociate. However, more than 90% of the substrate initially bound in such complexes dissociated before degradation. The experiment shown in Figure 5 was performed at 20°C. Parallel experiments performed at 30°C revealed no protection by SspB against competition by the second substrate (data not shown). These experiments suggest that complexes of ClpXP, SspB, and ssrA-tagged substrates are highly dynamic and thus largely uncommitted to degradation under physiological conditions. Because some commitment to degradation is observed, however, these experiments also demonstrate that complexes of ClpXP, SspB, and ssrA-tagged GFP are on pathway.

## Discussion

The results reported here show that SspB forms a stable dimer that binds two ssrA-tagged peptides or proteins. SspB by itself binds to ClpX and stimulates ATP hydrolysis by this enzyme. We have also shown that a complex containing one SspB dimer and two GFP-ssrA molecules assembles with a single ClpX hexamer to form a ternary complex in the presence of ATPγS. In the presence of ClpP and ATP, this ternary complex is competent in the sense that some bound ssrA-tagged substrates could be degraded without dissociation and rebinding.

In the presence of SspB, ClpX bound more tightly to ssrA-tagged proteins or peptides. This result provides a simple explanation for the observation that, at low substrate concentrations, SspB improves the efficiency of ClpXP-mediated degradation of ssrA-tagged molecules. This effect is probably physiologically important as SsrA-mediated tagging occurs when translation of a

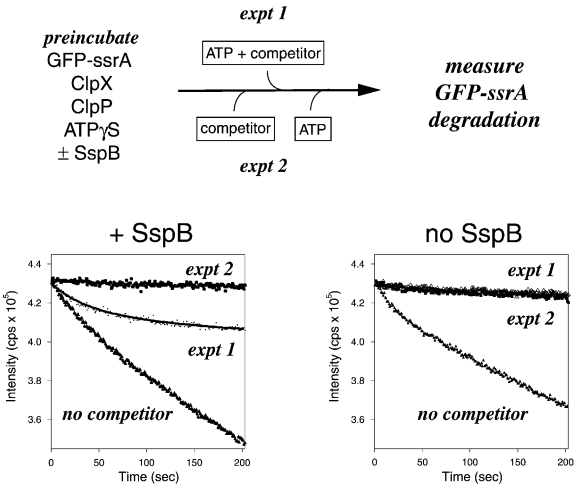


Figure 5. Competition Assays

$ClpX_6$ (1 μM), $ClpP_{14}$ (1.5 μM), GFP-ssrA (2.0 μM), and ATPγS (1 mM) were preincubated for 5 min at 30°C in the presence or absence of $SspB_2$ (1 μM). In experiment 1, ATP (7.5 mM) plus the Arc-ssrA competitor (50 μM) were added together at time zero, and degradation of GFP-ssrA was monitored by fluorescence. Experiment 2 was performed in the same way, except for inclusion of the Arc-ssrA competitor in the preincubation reaction. Control experiments performed under the same conditions but with no added competitor are also shown.

particular mRNA molecule is compromised, and thus most ssrA-tagged proteins are produced at relatively low concentrations in the cell [32]. Indeed, ssrA-tagged substrates have longer half-lives in *sspB*$^-$ cells than in *sspB*$^+$ cells [21].

In addition to its effects on substrate binding, SspB also increases the maximum rate of ClpXP degradation of ssrA-tagged protein [21, 22]. There are several potential explanations for this effect. First, we found that SspB can bind directly to ClpX and increase the rate at which this enzyme hydrolyzes ATP. In a similar fashion, SspB interactions with ClpX might enhance the ability of the enzyme to denature ssrA-tagged substrates. Second, $V_{max}$ might be increased to some extent because SspB is able to deliver two ssrA-tagged substrates to ClpX at once. Finally, denaturation of a single substrate molecule by ClpX is known to be an inefficient process that requires many catalytic cycles and the hydrolysis of roughly 150 molecules of ATP [20]. This probably occurs because substrates are loosely bound, and the application of force by ClpX leads to substrate dissociation more often than substrate unfolding. By this model, SspB could stabilize binding of the ssrA-tagged substrate, thereby increasing the probability of denaturation relative to dissociation.

Previous studies have shown that the 11-residue ssrA tag contains distinct sets of recognition determinants for SspB and ClpX [21, 22]. Specifically, SspB recognizes determinants in the seven N-terminal residues of the ssrA tag, whereas ClpX recognizes determinants in the three C-terminal residues. It has been proposed that ClpX initiates unfolding of ssrA-tagged substrates by engaging the tag [13, 19, 22]. If application of a pulling force to the very C terminus of the tag occurred in complexes with SspB and ClpX, then this should weaken the nearby interactions of the tag with SspB and might lead to more rapid dissociation of SspB. It is also possible that the thermodynamic stability of the SspB dimer allows it to withstand denaturation forces transmitted from ClpX through the bound ssrA-tagged substrate. In this regard, it is interesting that our experiments show that SspB binds ClpX as well or better than most substrates and, yet, is not itself a substrate for unfolding or degradation.

Our studies confirm that the ssrA tag does not need to be attached to a native protein to allow binding by SspB. Specifically, an 18-residue peptide ending with the ssrA tag bound with roughly micromolar affinity to SspB. On the other hand, SspB bound to native GFP-ssrA about 15-fold more tightly than to the ssrA peptide. This difference might result from an adventitious contact between the native portion of GFP-ssrA and SspB, but this explanation is not supported by the thermodynamics of binding. In particular, binding of the ssrA peptide to SspB had a more favorable enthalpy, whereas binding of native GFP-ssrA showed a significantly reduced entropic cost (Table 1). The opposite result would be expected for the simplest form of the adventitious-contact model. It is possible that it is more difficult for the ssrA tag to assume its proper SspB binding conformation when attached to a denatured protein. This could occur, for example, if interactions between the C terminus of the tag, which is quite hydrophobic, and other parts of

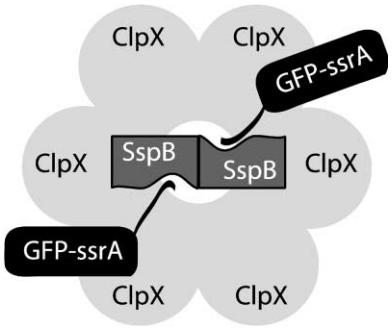


Figure 6. Model of the Complex of ClpX, SspB, and ssrA-Tagged Substrates

In the model, the 6-fold rotational axis of the ClpX hexamer is aligned with the presumed 2-fold axis of the SspB dimer. A single ssrA-tagged substrate is bound to each SspB subunit and is positioned to interact with ClpX.

an unstructured polypeptide chain had to be disrupted before the tag could fold into an SspB binding conformation. By this model, the ssrA peptide used here might be a good model for a denatured ssrA-tagged protein. It will be interesting to determine if SspB shows a generally greater affinity for native ssrA-tagged proteins than for denatured ssrA-tagged proteins. If so, SspB might preferentially deliver ssrA substrates that require active unfolding to ClpXP, leaving globally unfolded ssrA-tagged substrates to be degraded in an SspB-independent fashion by proteases such as ClpAP. It has been established that ClpAP can degrade denatured proteins without degradation tags [33], but ClpXP does not have this capability [34].

ClpX assembles as a hexameric ring with a central pore along its 6-fold rotational axis [6, 35]. In a ternary complex with maximal symmetry, the 6-fold of $ClpX_6$ would be aligned with a 2-fold axis of the $SspB_2$•GFP-$ssrA_2$ complex. In this arrangement, one ClpX trimer would interact with one SspB•GFP-ssrA unit (Figure 6), which, in turn, raises the possibility that each trimer may form a functional substructure within the hexamer. Indeed, in one crystal form of the related ATPase HslU (ClpY), the hexamer can be viewed as a dimer of trimers with each trimer containing two nucleotide-bound subunits and one nucleotide-free subunit [36]. Other HslU crystal forms, however, contain three or six bound nucleotides or inhibitors [9, 36–40], pointing to dimers or monomers as the fundamental repeat [41]. It will be important to determine how ATP binding and hydrolysis by different subunits of ClpX are mechanistically linked to SspB-mediated unfolding of ssrA-tagged substrates.

Several specificity factors and activity modulators for AAA+ ATPases have now been described, although to differing degrees of biochemical detail. Comparing these protein factors reveals many differences but some common principles. In certain cases, cofactor binding appears to redirect the AAA+ ATPase from one functional pathway to another, but there is no evidence that these modulators participate directly in substrate choice. For example, ClpS inhibits degradation of ssrA-tagged substrates by ClpAP and stimulates degradation of protein aggregates [23]. However, ClpS has no affinity

for ssrA-tagged substrates or protein aggregates and binds to a domain of ClpA that is not required for degradation of ssrA-tagged molecules [23, 42]. Unlike SspB, six ClpS monomers bind to one ClpA hexamer [23].

Other AAA+ modulators like SspB are actively involved in substrate selection. For example, MecA dimers bind to the ComK substrate and form ternary complexes with the ClpC ATPase [26, 43, 44]. Like SspB, MecA stimulates the ATPase activity of ClpC [26, 44]. However, unlike SspB, MecA is degraded together with ComK by the ClpCP protease [45]. A phosphorylated form of the RssB protein forms a 1:1 complex with the stationary-phase transcription factor, $\sigma^S$, and is required for degradation of this substrate by ClpXP [24, 25, 46–49]. In the presence of ATP$\gamma$S, a stable quaternary complex including ClpX, ClpP, RssB, and $\sigma^S$ is formed [49]. The subunit compositions of the ClpC•MecA•ComK and ClpX•RssB•$\sigma^S$ complexes have not been reported. A common stoichiometry of 6:2:2 between these systems and ClpX•SspB•GFP-ssrA is possible, however, and would be highly suggestive that ATPase trimers play a functionally significant role in substrate processing.

## Significance

**The study of the mechanisms by which accessory factors modulate the activity of AAA+ ATPases is becoming increasingly important in understanding chaperone and protease function. The results reported here provide a foundation for a mechanistic dissection of SspB, a specificity factor for the ATP-dependent ClpXP protease, which stimulates proteolysis of protein substrates bearing the ssrA degradation tag. Stable SspB homodimers bind two ssrA-tagged proteins or peptides and assemble with one ClpX hexamer to form a stable ternary complex in the presence of the ATP$\gamma$S. This complex is competent for GFP-ssrA degradation in the presence of ClpP and ATP. Although SspB does not kinetically commit bound ssrA-tagged substrates to ClpXP degradation, it permits more efficient degradation at low substrate concentrations by stabilizing and increasing the cooperativity of binding. SspB also increases the maximum rate of degradation, potentially by stimulating ClpX ATPase activity, delivering multiple substrates, and/or by stabilizing substrate interactions with ClpX. Our definition of conditions that allow isolation of stable ternary complexes should set the stage for structural studies of this macromolecular assembly.**

## Experimental Procedures

### Buffers

PD buffer contains 25 mM HEPES-KOH (pH 7.6), 5 mM KCl, 5 mM $MgCl_2$, 0.032% NP-40, and 10% glycerol. The ATP regenerating system consists of 4 mM ATP, 16 mM creatine phosphate, and 0.32 mg/ml creatine kinase. TC buffer contains 50 mM HEPES-KOH (pH 7.6), 200 mM KCl, 10 mM $MgCl_2$, 0.1 mM $ZnSO_4$, 2 mM DTT, 10% glycerol, and 1 mM ATP$\gamma$S.

### Proteins and Peptides

*E. coli* SspB, GFP-ssrA, and *E. coli* ClpX were expressed and purified as described [12, 21, 50]. Arc-ssrA was a gift of Randall Burton. The ssrA peptide ($NH_2$-NKKGRHGAANDENYALAA-COOH) was synthesized by the MIT Biopolymers Laboratory, desalted, and purified by reverse-phase chromatography on an LC-10AD-VP HPLC column (Shimadzu Corporation, Kyoto, Japan). The peptide was labeled with BODIPY-FL, CASE (Molecular Probes, Eugene, Oregon) using a standard protocol for labeling of amino groups. The BODIPY-labeled peptide was purified by reverse-phase HPLC and lyophilized. Concentrations of SspB monomers ($\epsilon_{280}$ = 12,090 $M^{-1}$ $cm^{-1}$), GFP-ssrA monomers ($\epsilon_{280}$ = 19,770 $M^{-1}$ $cm^{-1}$), and ClpX hexamers ($\epsilon_{280}$ = 84,480 $M^{-1}$ $cm^{-1}$) were determined by UV absorbance.

### Hydrodynamic Studies

Protein samples were centrifuged in an Optima XL-A centrifuge (Beckman-Coulter, Fullerton, California) using a 60 Ti rotor. SspB at 25, 41, or 66 $\mu$M in 25 mM MES (pH 6.0), 175 mM KCl, and 5% glycerol was centrifuged at 20°C at 8,000, 12,000, and 16,000 rpm. Absorbance readings were taken at 245, 280, and 285 nm. SspB at 2.5 and 10 $\mu$M in 25 mM HEPES-KOH (pH 7.6), 200 mM KCl, 1 mM DTT, and 10% glycerol was centrifuged at 4°C and 20°C at 8,000 and 12,000 rpm, respectively, and absorbance scans were taken at 230, 236, and 276 nm. SspB plus GFP-ssrA at 3, 6, and 10 $\mu$M monomer equivalents each in TC buffer minus ATP$\gamma$S were centrifuged at 4°C at 8,000, 12,000, and 16,000 rpm, and absorbance readings were taken at 276, 490, and 492 nm. For denaturation experiments, SspB at 3 and 15 $\mu$M in 10 mM potassium phosphate (pH 7.5); 200 mM KCl; and 2.6, 3.2, or 3.5 M GuHCl was centrifuged at 25°C at 16,000 rpm, and absorbance scans were taken at 230, 236, and 276 nm. Absorbance measurements were made at 3–4 hr intervals until equilibrium was reached (usually 24 hr). Scans were analyzed as described [51] to determine apparent molecular weights. In velocity sedimentation experiments, SspB (6 $\mu$M), GFP-ssrA (6 $\mu$M), and $ClpX_6$ (3 $\mu$M) in TC buffer plus 9 mM ATP$\gamma$S were centrifuged at 4°C at 40,000 rpm for 4 hr. Scans monitoring GFP-ssrA absorbance at 492 nm were taken every 2 min. Scans were analyzed using the time derivative method [31] using Origin (Microcal, Amherst, Massachusetts) to determine the sedimentation coefficient.

Dynamic-light scattering experiments were performed on DynaPro-MS/X (Protein Solutions). SspB and GFP-ssrA (6 $\mu$M monomer equivalents) were incubated for 5 min in TC buffer. $ClpX_6$ (3 $\mu$M) was added and incubated for 20 min, and the sample was spin filtered using a 0.2 $\mu$m filter. Four sets of 40 data points were collected and each data set was analyzed using the DYNAMICS software (Protein Solutions).

### Denaturation and Binding Assays

Curve fitting for denaturation and binding assays was performed in Kaleidagraph (Synergy Software, Reading, Pennsylvania). Fluorescence experiments were performed at 25°C using a QM-2000-4SE spectrofluorometer (Photon Technology International, London, Ontario) or a Fluoromax-2 instrument (ISA, Jobin-Yvon, Longjumeau, France). Fluorescence emission spectra of 15 $\mu$M SspB in 25 mM Tris-HCl (pH 7.6), 200 mM KCl, and 5% glycerol with or without 5 M GuHCl was measured by exciting the samples at 285 nm and recording spectra at 1 nm wavelengths with an integration time of 5 s. For denaturation experiments, SspB samples were prepared at each GuHCl concentration in 50 mM HEPES-KOH (pH 7.6), 200 mM KCl, and 1 mM DTT and incubated for at least 30 min. The GuHCl concentration was determined by refractive index using a Bausch & Lomb refractometer. Samples were incubated in a 25°C bath for 5 min immediately prior to measurement. Emission intensity was measured at 333 nm (excitation at 265 nm) for 60 s (1 s integration time) and averaged. Emission spectra were also measured from 300 to 400 nm, and the center of mass of the spectral peak was calculated. GuHCl denaturation of SspB was reversible as judged by the recovery of center of mass from dilution of the 4 M GuHCl sample to 2 M GuHCl.

Steady-state ATP hydrolysis by ClpX in the presence of SspB at 30°C was measured using a coupled assay [52] on a Spectramax Plus spectrometer (Molecular Devices). A 47.5 $\mu$l mixture of 0.3 $\mu$M $ClpX_6$, different quantities of SspB, 1 mM NADH, 2 mM phosphoenolpyruvate, 3 U/ml lactate dehydrogenase, and 3 U/ml pyruvate kinase in PD buffer plus 70 mM KCl was incubated in a 50 $\mu$M cuvette for 4 min. At this time, 2.5 $\mu$l of 100 mM ATP was added and loss of absorbance was monitored at 340 nm for 5 min. The rate of ADP

formation was calculated assuming a 1:1 correspondence between ATP regeneration and NADH oxidation and a $\Delta\epsilon_{340}$ of 6.23 $\mu M^{-1}$ $cm^{-1}$ [52].

Binding at 25°C was assayed by isothermal titration calorimetry in 10 mM Tris-HCl (pH 7.6) and 50 mM KCl, using a VP-ITC calorimeter (Microcal) equipped with a 300 μl syringe. SspB (195 μM or 175 μM) was loaded into the syringe and injected in 7.5 μl volumes at 320 s intervals into a 1.3 ml cell containing either the ssrA peptide (15 μM) or GFP-ssrA (14 μM). Samples were degassed prior to measurement. Baseline corrections, integration, and least-squares fitting were performed with Origin software (Microcal). Typically, the first two to three data points were discarded, and the average of the following baseline points was entered into the final data evaluation.

Binding of SspB, ClpX, and mixtures of SspB and ClpX to the BODIPY-labeled ssrA peptide (50 nM) was assayed by fluorescence anisotropy (excitation 477 nm, emission 511 nm) at 20°C and 30°C in 50 mM HEPES-KOH (pH 7.6), 44 mM Tris-HCl, 200 mM KCl, 10 mM $MgCl_2$, 10% glycerol, 2 mM DTT, and 10 mM ATPγS. Assays to monitor degradation of GFP-ssrA were performed at 30°C using 0.3 μM $ClpX_6$ and 0.8 μM $P_{14}$ in PD buffer plus 200 mM KCl and the ATP regenerating system. GFP-ssrA (9.4 nM to 4.8 μM in 2-fold increments plus 7.2 and 9.0 μM) or mixtures of GFP-ssrA and SspB (9.4 nM to 4.8 μM monomer equivalents in 2-fold increments) were preincubated at 30°C and added to the ClpXP mixture. Samples were excited at 467 nm and monitored at 511 nm for 10 min.

Competition assays contained 50 mM HEPES-KOH (pH 7.6), 44 mM Tris-HCl, 200 mM KCl, 110 mM NaCl, 10 mM $MgCl_2$, 10% glycerol, and 1 mM DTT. $SspB_2$ (1 μM), GFP-$ssrA_2$ (1 μM), $ClpX_6$ (1 μM), $ClpP_{14}$ (1.5 μM), and ATPγS (1 mM) were preincubated at 30°C in the presence or absence of 50 μM Arc-ssrA. Prewarmed ATP (7.5 mM) or ATP plus 50 μM Arc-ssrA was added, and degradation was assayed by changes in fluorescence (excitation 467 nm, emission 511 nm).

### Chromatography

Gel-filtration and ion-exchange chromatography was performed on a SMART System (Amersham Biosciences) using Superdex 200 and MonoQ PC 1.6/5 columns. For gel filtration, the column was equilibrated in TC buffer at 4°C. SspB and GFP-ssrA (6 μM monomer equivalents) were incubated in TC buffer plus 4 mM ATPγS for 5 min. After this time, different quantities of $ClpX_6$ (0.7 μM, 1.4 μM, 2.1 μM, 2.8 μM, 4.2 μM, and 5.6 μM) were added in separate experiments and incubated for an additional 20 min before loading onto the column. For ion exchange, the column was equilibrated in TC buffer at 4°C, and a gradient was run from 200–350 mM KCl. SspB and GFP-ssrA (6 μM monomer equivalents) and $ClpX_6$ (3 μM) were prepared in the same manner as for gel filtration. GFP-ssrA absorbance was monitored, and two fractions (200 μL) from the single peak containing the ternary complex were pooled, added to 200 μl of 0.06% trifluoroacetic acid (v/v), and centrifuged. Separation of the three proteins was performed on an LC-10AD-VP HPLC (Shimadzu) using a C4 reverse phase column, with a gradient from 0%–80% acetonitrile (v/v) in 0.06% trifluoroacetic acid over 70 min. Elution was monitored at 214 and 280 nm, and peaks were integrated in CLASS-VP software (Shimadzu).

### Acknowledgments

We thank members of the Sauer and Baker labs for technical support and advice, and the Multi-user Facility for the Study of Complex Molecular Systems (NSF-0070319) as well as the Bell and Stern labs for use of equipment. This work was supported by a grant from the National Institutes of Health (AI-16892). D.A.W. is a Cissy Hornung American Cancer Society Postdoctoral Fellow. I.L. and T.A.B. are employees of the Howard Hughes Medical Institute.

Received: August 23, 2002
Revised: October 2, 2002
Accepted: October 2, 2002

### References

1. Schmidt, M., Lupas, A.N., and Finley, D. (1999). Structure and mechanism of ATP-dependent proteases. Curr. Opin. Chem. Biol. *3*, 584–591.
2. Ogura, T., and Wilkinson, A.J. (2001). AAA+ superfamily ATPases: common structure–diverse function. Genes Cells *6*, 575–597.
3. Kessel, M., Maurizi, M.R., Kim, B., Kocsis, E., Trus, B.L., Singh, S.K., and Steven, A.C. (1995). Homology in structural organization between *E. coli* ClpAP protease and the eukaryotic 26 S proteasome. J. Mol. Biol. *250*, 587–594.
4. Bochtler, M., Ditzel, L., Groll, M., and Huber, R. (1997). Crystal structure of heat shock locus V (HslV) from *Escherichia coli*. Proc. Natl. Acad. Sci. USA *94*, 6070–6074.
5. Wang, J., Hartling, J.A., and Flanagan, J.M. (1997). The structure of ClpP at 2.3 Å resolution suggests a model for ATP-dependent proteolysis. Cell *91*, 447–456.
6. Grimaud, R., Kessel, M., Beuron, F., Steven, A.C., and Maurizi, M.R. (1998). Enzymatic and structural similarities between the *Escherichia coli* ATP-dependent proteases, ClpXP and ClpAP. J. Biol. Chem. *273*, 12476–12481.
7. Bochtler, M., Ditzel, L., Groll, M., Hartmann, C., and Huber, R. (1999). The proteasome. Annu. Rev. Biophys. Biomol. Struct. *28*, 295–317.
8. Voges, D., Zwickl, P., and Baumeister, W. (1999). The 26S proteasome: a molecular machine designed for controlled proteolysis. Annu. Rev. Biochem. *68*, 1015–1068.
9. Sousa, M.C., Trame, C.B., Tsuruta, H., Wilbanks, S.M., Reddy, V.S., and McKay, D.B. (2000). Crystal and solution structures of an HslUV protease-chaperone complex. Cell *103*, 633–643.
10. Unno, M., Mizushima, T., Morimoto, Y., Tomisugi, Y., Tanaka, K., Yasuoka, N., and Tsukihara, T. (2002). The structure of the mammalian 20S proteasome at 2.75 Å resolution. Structure *10*, 609–618.
11. Laachouch, J.E., Desmet, L., Geuskens, V., Grimaud, R., and Toussaint, A. (1996). Bacteriophage Mu repressor as a target for the *Escherichia coli* ATP-dependent Clp Protease. EMBO J. *15*, 437–444.
12. Levchenko, I., Yamauchi, M., and Baker, T.A. (1997). ClpX and MuB interact with overlapping regions of Mu transposase: implications for control of the transposition pathway. Genes Dev. *11*, 1561–1572.
13. Gottesman, S., Roche, E., Zhou, Y., and Sauer, R.T. (1998). The ClpXP and ClpAP proteases degrade proteins with carboxy-terminal peptide tails added by the SsrA-tagging system. Genes Dev. *12*, 1338–1347.
14. Gonzalez, M., Frank, E.G., Levine, A.S., and Woodgate, R. (1998). Lon-mediated proteolysis of the *Escherichia coli* UmuD mutagenesis protein: *in vitro* degradation and identification of residues required for proteolysis. Genes Dev. *12*, 3889–3899.
15. Gonciarz-Swiatek, M., Wawrzynow, A., Um, S.J., Learn, B.A., McMacken, R., Kelley, W.L., Georgopoulos, C., Sliekers, O., and Zylicz, M. (1999). Recognition, targeting, and hydrolysis of the λ O replication protein by the ClpP/ClpX protease. J. Biol. Chem. *274*, 13999–14005.
16. Tu, G.F., Reid, G.E., Zhang, J.G., Moritz, R.L., and Simpson, R.J. (1995). C-terminal extension of truncated recombinant proteins in *Escherichia coli* with a 10Sa RNA decapeptide. J. Biol. Chem. *270*, 9322–9326.
17. Keiler, K.C., Waller, P.R., and Sauer, R.T. (1996). Role of a peptide tagging system in degradation of proteins synthesized from damaged messenger RNA. Science *271*, 990–993.
18. Weber-Ban, E.U., Reid, B.G., Miranker, A.D., and Horwich, A.L. (1999). Global unfolding of a substrate protein by the Hsp100 chaperone ClpA. Nature *401*, 90–93.
19. Kim, Y.I., Burton, R.E., Burton, B.M., Sauer, R.T., and Baker, T.A. (2000). Dynamics of substrate denaturation and translocation by the ClpXP degradation machine. Mol. Cell *5*, 639–648.
20. Burton, R.E., Siddiqui, S.M., Kim, Y.I., Baker, T.A., and Sauer, R.T. (2001). Effects of protein stability and structure on substrate processing by the ClpXP unfolding and degradation machine. EMBO J. *20*, 3092–3100.
21. Levchenko, I., Seidel, M., Sauer, R.T., and Baker, T.A. (2000). A

specificity-enhancing factor for the ClpXP degradation machine. Science *289*, 2354–2356.
22. Flynn, J.M., Levchenko, I., Seidel, M., Wickner, S.H., Sauer, R.T., and Baker, T.A. (2001). Overlapping recognition determinants within the ssrA degradation tag allow modulation of proteolysis. Proc. Natl. Acad. Sci. USA *98*, 10584–10589.
23. Dougan, D.A., Reid, B.G., Horwich, A.L., and Bukau, B. (2002). ClpS, a substrate modulator of the ClpAP machine. Mol. Cell *9*, 673–683.
24. Muffler, A., Fischer, D., Altuvia, S., Storz, G., and Hengge-Aronis, R. (1996). The response regulator RssB controls stability of the $\sigma^s$ subunit of RNA polymerase in *Escherichia coli*. EMBO J. *15*, 1333–1339.
25. Pratt, L.A., and Silhavy, T.J. (1996). The response regulator SprE controls the stability of RpoS. Proc. Natl. Acad. Sci. USA *93*, 2488–2492.
26. Turgay, K., Hamoen, L.W., Venema, G., and Dubnau, D. (1997). Biochemical characterization of a molecular switch involving the heat shock protein ClpC, which controls the activity of ComK, the competence transcription factor of *Bacillus subtilis*. Genes Dev. *11*, 119–128.
27. Kondo, H., Rabouille, C., Newman, R., Levine, T.P., Pappin, D., Freemont, P., and Warren, G. (1997). p47 is a cofactor for p97-mediated membrane fusion. Nature *388*, 75–78.
28. Meyer, H.H., Shorter, J.G., Seemann, J., Pappin, D., and Warren, G. (2000). A complex of mammalian Ufd1 and Npl4 links the AAA-ATPase, p97, to ubiquitin and nuclear transport pathways. EMBO J. *19*, 2181–2192.
29. Ye, Y., Meyer, H.H., and Rapoport, T.A. (2001). The AAA ATPase Cdc48/p97 and its partners transport proteins from the ER into the cytosol. Nature *414*, 652–656.
30. Hetzer, M., Meyer, H.H., Walther, T.C., Bilbao-Cortes, D., Warren, G., and Mattaj, I.W. (2001). Distinct AAA-ATPase p97 complexes function in discrete steps of nuclear assembly. Nat. Cell Biol. *3*, 1086–1091.
31. Stafford, W.F., 3rd. (1992). Boundary analysis in sedimentation transport experiments: a procedure for obtaining sedimentation coefficient distributions using the time derivative of the concentration profile. Anal. Biochem. *203*, 295–301.
32. Roche, E.D., and Sauer, R.T. (2001). Identification of endogenous SsrA-tagged proteins reveals tagging at positions corresponding to stop codons. J. Biol. Chem. *276*, 28509–28515.
33. Hoskins, J.R., Singh, S.K., Maurizi, M.R., and Wickner, S. (2000). Protein binding and unfolding by the chaperone ClpA and degradation by the protease ClpAP. Proc. Natl. Acad. Sci. USA *97*, 8892–8897.
34. Singh, S.K., Grimaud, R., Hoskins, J.R., Wickner, S., and Maurizi, M.R. (2000). Unfolding and internalization of proteins by the ATP-dependent proteases ClpXP and ClpAP. Proc. Natl. Acad. Sci. USA *97*, 8898–8903.
35. Ortega, J., Singh, S.K., Ishikawa, T., Maurizi, M.R., and Steven, A.C. (2000). Visualization of substrate binding and translocation by the ATP-dependent protease, ClpXP. Mol. Cell *6*, 1515–1521.
36. Bochtler, M., Hartmann, C., Song, H.K., Bourenkov, G.P., Bartunik, H.D., and Huber, R. (2000). The structures of HslU and the ATP-dependent protease HslU-HslV. Nature *403*, 800–805.
37. Song, H.K., Hartmann, C., Ramachandran, R., Bochtler, M., Behrendt, R., Moroder, L., and Huber, R. (2000). Mutational studies on HslU and its docking mode with HslV. Proc. Natl. Acad. Sci. USA *97*, 14103–14108.
38. Wang, J., Song, J.J., Franklin, M.C., Kamtekar, S., Im, Y.J., Rho, S.H., Seong, I.S., Lee, C.S., Chung, C.H., and Eom, S.H. (2001). Crystal structures of the HslVU peptidase-ATPase complex reveal an ATP-dependent proteolysis mechanism. Structure *9*, 177–184.
39. Trame, C.B., and McKay, D.B. (2001). Structure of Haemophilus influenzae HslU protein in crystals with one-dimensional disorder twinning. Acta Crystallogr. D Biol. Crystallogr. *57*, 1079–1090.
40. Sousa, M.C., Kessler, B.M., Overkleeft, H.S., and McKay, D.B. (2002). Crystal structure of HslUV complexed with a vinyl sulfone inhibitor: corroboration of a proposed mechanism of allosteric activation of HslV by HslU. J. Mol. Biol. *318*, 779–785.
41. Wang, J., Song, J.J., Seong, I.S., Franklin, M.C., Kamtekar, S., Eom, S.H., and Chung, C.H. (2001). Nucleotide-dependent conformational changes in a protease-associated ATPase HslU. Structure *9*, 1107–1116.
42. Lo, J.H., Baker, T.A., and Sauer, R.T. (2001). Characterization of the N-terminal repeat domain of *Escherichia coli* ClpA-A class I Clp/HSP100 ATPase. Protein Sci. *10*, 551–559.
43. Liu, L., Nakano, M.M., Lee, O.H., and Zuber, P. (1996). Plasmid-amplified *comS* enhances genetic competence and suppresses *sinR* in *Bacillus subtilis*. J. Bacteriol. *178*, 5144–5152.
44. Persuh, M., Turgay, K., Mandic-Mulec, I., and Dubnau, D. (1999). The N- and C-terminal domains of MecA recognize different partners in the competence molecular switch. Mol. Microbiol. *33*, 886–894.
45. Turgay, K., Hahn, J., Burghoorn, J., and Dubnau, D. (1998). Competence in *Bacillus subtilis* is controlled by regulated proteolysis of a transcription factor. EMBO J. *17*, 6730–6738.
46. Zhou, Y., and Gottesman, S. (1998). Regulation of proteolysis of the stationary-phase sigma factor RpoS. J. Bacteriol. *180*, 1154–1158.
47. Becker, G., Klauck, E., and Hengge-Aronis, R. (1999). Regulation of RpoS proteolysis in *Escherichia coli*: the response regulator RssB is a recognition factor that interacts with the turnover element in RpoS. Proc. Natl. Acad. Sci. USA *96*, 6439–6444.
48. Klauck, E., Lingnau, M., and Hengge-Aronis, R. (2001). Role of the response regulator RssB in $\sigma^S$ recognition and initiation of $\sigma^S$ proteolysis in *Escherichia coli*. Mol. Microbiol. *40*, 1381–1390.
49. Zhou, Y., Gottesman, S., Hoskins, J.R., Maurizi, M.R., and Wickner, S. (2001). The RssB response regulator directly targets $\sigma^S$ for degradation by ClpXP. Genes Dev. *15*, 627–637.
50. Yakhnin, A.V., Vinokurov, L.M., Surin, A.K., and Alakhov, Y.B. (1998). Green fluorescent protein purification by organic extraction. Protein Expr. Purif. *14*, 382–386.
51. Laue, T.M., Shah, B.D., Ridgeway, T.M., and Pelletier, S.L. (1992). Computer-aided interpretation in biochemistry and polymer science. In Analytical Ultracentrifugation in Biochemistry and Polymer Science, S. Harding, A. Rowe and J. Horton, eds. (Cambridge, UK: Royal Society of Chemistry), pp. 90–125.
52. Nørby, J.G. (1988). Coupled assay of Na+,K+-ATPase activity. Methods Enzymol. *156*, 116–119.